

Generalized Parton Distributions from Lattice QCD

Dru B. Renner

Department of Physics, University of Arizona, 1118 E 4th Street, Tucson, AZ 85721, USA

Abstract. I review the LHPC Collaboration's lattice QCD calculations of the generalized parton distributions of the nucleon and highlight those aspects of nucleon structure best illuminated by lattice QCD, the nucleon's spin decomposition and transverse quark structure.

1. Introduction

Generalized parton distributions provide the means to calculate aspects of nucleon structure not previously accessible to lattice QCD calculations. Primary among these are the nucleon spin decomposition [1] and the transverse quark structure [2]. The generalized parton distributions determine the fraction of nucleon spin carried by quark helicity, quark orbital motion, and gluons. Additionally, the generalized parton distributions provide a three dimensional picture of a fast moving nucleon by extending the ordinary parton distributions into the transverse plane.

The Lattice Hadron Physics Collaboration is pursuing a program to calculate the nucleon's generalized parton distributions. Initial calculations have been completed for pion masses from 750 MeV to 900 MeV [3, 4]. Additionally current calculations are underway covering the region of pion masses from 350 MeV to 750 MeV [5]. In these proceedings I review the results from our earlier calculations highlighting the potential impact of lattice QCD calculations on our understanding of quark orbital motion and transverse quark structure within the nucleon.

2. Generalized Form Factors

Definitions of the generalized parton distributions can be found in [6]. However, there is an equivalent and more convenient language which is naturally suited to lattice calculations, generalized form factors. The generalized form factors are defined in terms of matrix elements of the twist two operators which can be calculated on the lattice. For example consider the tower of twist two operators $O_q^{\mu_1 \dots \mu_n} = \bar{q} i D^{(\mu_1} \dots i D^{\mu_{n-1}} \gamma^{\mu_n)} q$. There is a corresponding tower of generalized form factors, A_{ni}^q , B_{ni}^q , and C_n^q , defined by

$$\langle P' | O_q^{\mu_1 \dots \mu_n} | P \rangle = \bar{U}(P') \left[\sum_{i=0, \text{even}}^{n-1} \left(A_{ni}^q(t) K_{ni}^A + B_{ni}^q(t) K_{ni}^B \right) + \delta_{\text{even}}^n C_n^q(t) K_n^C \right] U(P) \quad (1)$$

where the K are kinematic functions of P and P' and the spin labels have been suppressed.

3. Lattice Calculation

The details of our lattice calculation are given in [7] and [3]. In brief, we calculate the matrix elements on the left hand side of equation 1 on the lattice. We then match these results to the \overline{MS} scheme at $\mu = 2$ GeV, and invert equation 1 to determine the generalized form factors. A

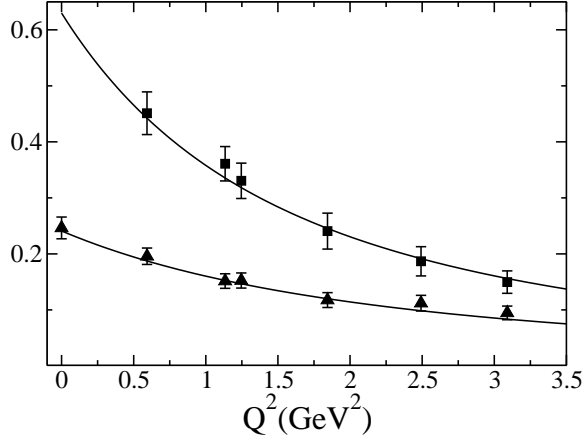


Figure 1. squares are B_{20}^{u-d} , triangles are A_{20}^{u-d}

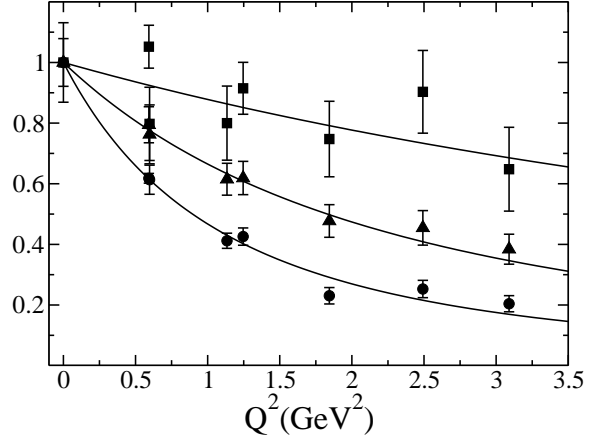


Figure 2. squares are A_{30}^{u-d} , triangles are A_{20}^{u-d} , circles are A_{10}^{u-d}

key feature of our method is that we calculate an exhaustive set of matrix elements and solve the resulting overdetermined system of equations to extract the generalized form factors with as small an error as possible. In the following I use only results from a single lattice calculation with $m_\pi = 896(6)$ MeV. Further details can be found in the references above. Additionally, there are other similar calculations in the literature [8, 9, 10, 11, 12].

4. Quark Orbital Motion

The nucleon spin can be written as the sum of three separately gauge invariant observables,

$$1/2 = 1/2 \Delta\Sigma^{u+d} + L^{u+d} + J^g, \quad (2)$$

where the terms from left to right are the contributions from the quark helicity, quark orbital angular momentum, and total gluon angular momentum. The observables in equation 2 are each given by singlet matrix elements which pose a significant challenge to lattice calculations. Singlet matrix elements require the computation of disconnected quark diagrams which are computationally quite demanding.

However non-singlet matrix elements receive no contributions from disconnected diagrams and are readily calculated on the lattice. In our calculation [13], shown in figure 1, we found that $L^{u-d} = -0.193(32)$ indicating that at least one of the quark flavors is undergoing significant orbital motion. This is quite interesting given that the connected contribution to L^{u+d} is $0.002(3)$ which, ignoring disconnected diagrams, suggests a strong cancellation among the quark flavors. Due to the missing contributions to L^{u+d} we are incapable of determining L^u and L^d separately, however, we can set a lower bound on the typical contribution from the quark orbital motion: the average magnitude of the quark orbital angular momentum, $L_{\text{ave}} = 1/2(|L^u| + |L^d|)$, is bounded from below, $L_{\text{ave}} \geq |L^{u-d}|$, indicating that on average the quarks are contributing, by way of their orbital motion, on the order of 20% of the nucleon's total spin.

5. Transverse Quark Structure

The transverse quark distribution, $q(x, \vec{b}_\perp)$, gives the probability to find a quark q with a momentum fraction x at a distance \vec{b}_\perp from the transverse center of the nucleon. The x moments of the transverse distribution are given by

$$q_n(\vec{b}_\perp) = \int_{-1}^1 dx x^{n-1} q(x, \vec{b}_\perp) = \int \frac{d^2\Delta_\perp}{(2\pi)^2} e^{-i\vec{b}_\perp \cdot \vec{\Delta}_\perp} A_{n0}^q(-\vec{\Delta}_\perp^2). \quad (3)$$

The Q^2 dependence of A_{n0}^q is calculated directly on the lattice and, as explained shortly, for large n probes the transverse distribution of quarks with x near 1. Specifically we calculate the transverse rms radius and average x of the distribution $\int dx x^{n-1} q(x, \vec{b}_\perp)$ allowing us to indirectly examine the x dependence of the transverse size of the nucleon. Additionally, upon entertaining a few assumptions, we can construct the \vec{b}_\perp dependence of $q(x, \vec{b}_\perp)$ as well. The details of the following calculations are given in [14] and [4].

5.1. Q^2 Dependence

The Q^2 dependence of, and in particular the slope of, A_{n0}^q determines the rms radius of the n^{th} moment of $q(x, \vec{b}_\perp)$,

$$\langle b_\perp^2 \rangle_n = \frac{\int d^2 b_\perp b_\perp^2 \int_{-1}^1 dx x^{n-1} q(x, \vec{b}_\perp)}{\int d^2 b_\perp \int_{-1}^1 dx x^{n-1} q(x, \vec{b}_\perp)} = \frac{-4}{A_{n0}^q(0)} \frac{dA_{n0}^q(0)}{dQ^2}. \quad (4)$$

Notice that for large n the integrals in equation 4 are dominated by the limit $x \rightarrow 1$. Furthermore, as $x \rightarrow 1$ a single quark carries all the longitudinal momentum of the nucleon. As discussed in [4], a quark in this limit is kinematically constrained to have $\vec{b}_\perp \rightarrow 0$. Additionally, explicit light cone wave functions show $q(x, \vec{b}_\perp)$ behaves as $\delta^2(\vec{b}_\perp)$ for $x \rightarrow 1$. Thus equation 4 demonstrates that the slope, and corresponding rms radius, of A_{n0}^q vanishes as $n \rightarrow \infty$. It is quite reassuring that we find, as shown in figure 2, that even for $n = 1, 2$, and 3 we see the slopes of A_{n0}^q decreasing with increasing n indicating that the transverse distribution of quarks within the nucleon is indeed becoming more narrow as x approaches 1.

5.2. x Dependence

The rms radii $\langle b_\perp^2 \rangle_n$ in equation 4 give the transverse size at a fixed moment n rather than at a fixed momentum fraction x ,

$$\langle b_\perp^2 \rangle_x = \frac{\int d^2 b_\perp b_\perp^2 q(x, \vec{b}_\perp)}{\int d^2 b_\perp q(x, \vec{b}_\perp)}.$$

However for a fixed n there is a region of x which dominates $\langle b_\perp^2 \rangle_n$, thus we can think of $\langle b_\perp^2 \rangle_n$ as an average of $\langle b_\perp^2 \rangle_x$ over a region centered on the average x of the n^{th} moment,

$$\langle x \rangle_n = \frac{\int d^2 b_\perp \int_{-1}^1 dx |x| x^{n-1} q(x, \vec{b}_\perp)}{\int d^2 b_\perp \int_{-1}^1 dx x^{n-1} q(x, \vec{b}_\perp)} = \frac{\langle x^n \rangle + 2(-1)^n \int d^2 b_\perp \int_0^1 dx x^n \bar{q}(x)}{\langle x^{n-1} \rangle} \approx \frac{\langle x^n \rangle}{\langle x^{n-1} \rangle}. \quad (5)$$

The anti-quark contribution in equation 5 is not accessible to current lattice calculations, however we expect it to be small and simple guesses based on the phenomenologically determined distributions indicated the following qualitative conclusion is not spoiled by ignoring it. In figure 3 we plot $\sqrt{\langle b_\perp^2 \rangle_n}$ versus $\langle x \rangle_n$ demonstrating that the transverse size of the nucleon again appears to depend significantly on the momentum fraction at which it is probed. Note that $\langle b_\perp^2 \rangle_2$ is not shown in the figure because $n = 2$ corresponds to the $q + \bar{q}$ distribution whereas $n = 1, 3$ correspond to the $q - \bar{q}$ distribution.

5.3. b_\perp Dependence

Lattice calculations of parton distributions are restricted to a few low moments, however equation 3 illustrates that the \vec{b}_\perp dependence of the lowest moments is quite illuminating. For $n = 1$ we have $\int dx q(x, \vec{b}_\perp)$ which is the transverse probability distribution without regard to the momentum fraction. Furthermore the corresponding operator is conserved, hence $q(\vec{b}_\perp)$

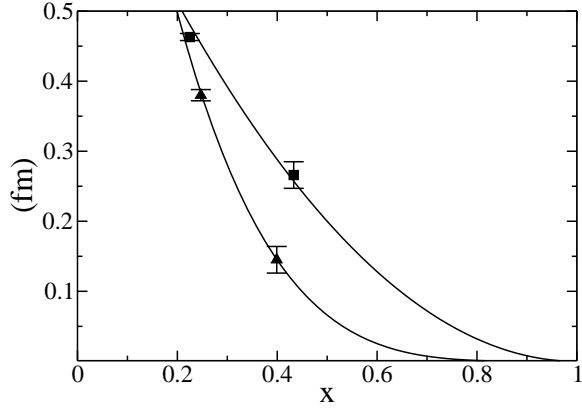


Figure 3. squares are $\langle b_{\perp}^2 \rangle_{(n)}^{u+d}$, triangles are $\langle b_{\perp}^2 \rangle_{(n)}^{u-d}$ for $n = 1, 3$

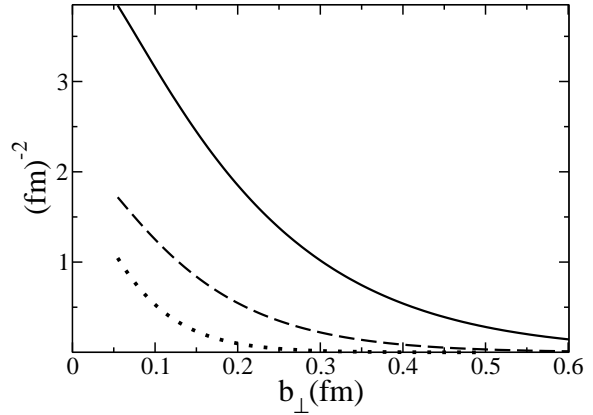


Figure 4. solid, dashed, dotted are $q_n(\vec{b}_{\perp})$ for $n = 1, 2, 3$, $q = u - d$

is independent of the renormalization scale. For $n = 2$ we have $\int dx x q(x, \vec{b}_{\perp})$ which is the transverse momentum distribution for which the sum over all quarks and gluons is again conserved and hence the total transverse momentum distribution is also scale independent. Unfortunately the moments $n \geq 3$ no longer have simple physical interpretations, nonetheless they represent the transverse distribution of the corresponding moment.

Assuming a dipole form for A_{n0}^q , which is justified by figure 2 for $Q^2 \leq 3.5\text{GeV}^2$, we can perform the integrals in equation 3 and calculate the \vec{b}_{\perp} dependence of each fixed moment for $b_{\perp}^2 \geq (3.5\text{GeV}^2)^{-1}$. As figure 4 illustrates we again observe that the lowest moment is the most broadly distributed in the transverse plane and higher moments are successively more narrow.

6. Conclusion

Our lattice calculations of the nucleon's generalized form factors have yielded insight into the quark structure of the nucleon. We have demonstrated that for a world with heavy pion masses the quark orbital motion constitutes roughly 20% of the nucleon's spin. Additionally we have shown, in several ways, that the transverse distribution of quarks within the nucleon depends significantly on the momentum fraction of the quarks. We are currently pursuing calculations with significantly lighter pion masses [5] in an effort to examine the quark substructure of the physical nucleon.

References

- [1] X. D. Ji, Phys. Rev. Lett. **78**, 610 (1997), hep-ph/9603249.
- [2] M. Burkardt, Phys. Rev. **D62**, 071503 (2000), hep-ph/0005108.
- [3] LHPC, P. Hagler *et al.*, Phys. Rev. **D68**, 034505 (2003), hep-lat/0304018.
- [4] LHPC, P. Hagler *et al.*, Phys. Rev. Lett. **93**, 112001 (2004), hep-lat/0312014.
- [5] LHPC, D. B. Renner *et al.*, (2004), hep-lat/0409130.
- [6] M. Diehl, Phys. Rept. **388**, 41 (2003), hep-ph/0307382.
- [7] LHPC, D. Dolgov *et al.*, Phys. Rev. **D66**, 034506 (2002), hep-lat/0201021.
- [8] QCDSF, M. Gockeler *et al.*, Phys. Rev. Lett. **92**, 042002 (2004), hep-ph/0304249.
- [9] QCSSF, M. Gockeler *et al.*, Nucl. Phys. Proc. Suppl. **128**, 203 (2004), hep-ph/0312104.
- [10] QCDSF, M. Gockeler *et al.*, (2004), hep-lat/0409162.
- [11] QCDSF, M. Gockeler *et al.*, (2004), hep-lat/0410023.
- [12] N. Mathur *et al.*, Phys. Rev. **D62**, 114504 (2000), hep-ph/9912289.
- [13] LHPC, J. W. Negele *et al.*, Nucl. Phys. Proc. Suppl. **129**, 910 (2004), hep-lat/0309060.
- [14] LHPC, W. Schroers *et al.*, Nucl. Phys. Proc. Suppl. **129**, 907 (2004), hep-lat/0309065.